A Study of the Liquid and Solvent Properties of Optically Active and Racemic α-Methylbenzylamine

Andrew T. Fischer,[†] Richard M. Pagni,*[,†] and Robert N. Compton[†,‡]

Departments of Chemistry and Physics, University of Tennessee, Knoxville, Tennessee 37996

Received: March 19, 2007; In Final Form: May 8, 2007

Speed-of-sound measurements are reported for *RS* (racemic) and *S* liquid α-methylbenzylamine (MBA) obtained using a modified design of previously published experimental geometry. After correcting for density changes, the resulting isentropic compressibility of the *S* liquid is found to be 2% larger than that of the *RS* racemic mixture. These data, along with proton NMR chemical shifts and published partial molar volumes, suggest that the structures of the racemic and optically active liquids are subtly different. The magnitude of the compressibilities and other data such as viscosity and the Kamlet−Taft parameters are consistent with the molecules in the liquids interacting via extensive hydrogen bonding. Cyclohexane, toluene, nitrobenzene, dimethyl sulfoxide, and methanol are completely miscible in MBA, as predicted from their corresponding Hildebrand solubility parameters. Proton NMR, optical rotation, and IR studies were carried out on solutions of the five solutes in MBA as a function of mole fraction. The asymmetric NH stretch of MBA was particularly informative in this regard. Solvation models were developed for the five solutes. The NH stretch frequency in cyclohexane changed only slightly up to a mole fraction of 0.7 in the hydrocarbon at which point the NH stretch greatly increased by about 200 cm^{-1} at a mole fraction of 1. The hydrogen-bonding network does not dissipate until there is at least 70 mol % cyclohexane in the MBA. Gaussian calcuations were also carried out to complement the ir studies.

Introduction

A majority of chemical and biochemical phenomena take place in solution. To understand in detail how these phenomena occur, it is necessary to comprehend the structure of liquids and how they interact with solute molecules.[1] α-Methylbenzylamine (MBA; 1-phenylethylamine) is an interesting liquid in this regard because it exists in optically active and racemic forms and belongs to a class of medically and biochemically important amines. A three-dimensional representation of the *R* enantiomer is shown below.

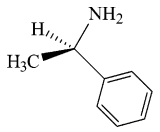

(*R*)-α-Methylbenzylamine

Given the structure, one would expect that hydrogen bonding and polarity to be important features of its liquid structure and solvation properties.

Numerous studies have been published which relate to MBA's structure. Of most importance to this study, the difference in partial molar volumes between the optically active and racemic forms has been determined in two separate studies.[2,3] The racemic form has a very slighty smaller molar volume than the optically active form (considerably less than 1%), which means that the racemic molecules pack slightly better in the liquid than do the optically active molecules. This is perhaps another manifestation of Wallach's rule which states that racemic molecules pack better in crystals than their optically active counterparts, although there are exceptions to the rule.[4] The enthalpy of mixing of the two enantiomers of MBA has been reported in two publications and is very slightly endothermic in both cases: +7.3 J/mol[5] and +9.06 J/mol,[6] both determined at 303.11K. Because the entropy of mixing of the two enantiomers is *R* ln 2, the free energy of the racemic liquid at 25 °C is lower than that of the *R* or *S* enantiomeric liquid by 1.7 kJ/mol. The enthalpy of vaporization of the *R*-, *S*-, and racemic MBA has also been determined,[7] the values of the three liquids being identical within the error of the measurement: 54.50 ± 0.08 kJ/mol. From the enthalpy of vaporization, one deduces[1] that the cohesive energy density of liquid MBA at 25 °C to be 405 MPa and the Hildebrand solubility parameter to be 20.1, a value intermediate between the extreme values of polar water and nonpolar perfluoroheptane. One thus expects that numerous solutes will be completely miscible with MBA, a prediction which is born out by experiment, as shown below. Our recent paper examined the specific rotation of the *S* enantiomer of MBA in a series of solvents.[8] The observed rotations were correlated with the Kamlet-Taft solvent parameters, α, β, and π^*.[8] The polarity, π^*, and acidity, α, of the solvent were found to have the greatest influence on MBA's rotations. β, the basicity of solvent, had the least effect on the rotations.

Herein we report the results of a series of experiments which probe in more detail the structure of liquid MBA and how it solvates a series of disparate solutes including methanol, dimethyl sulfoxide, cyclohexane, toluene, and nitrobenzene. The techniques used in this investigation were speed of sound measurements on optically active and racemic MBA, infrared

* Corresponding author.
[†] Department of Chemistry.
[‡] Department of Physics.

10.1021/jp072174+ CCC: $37.00 © 2007 American Chemical Society
Published on Web 06/21/2007

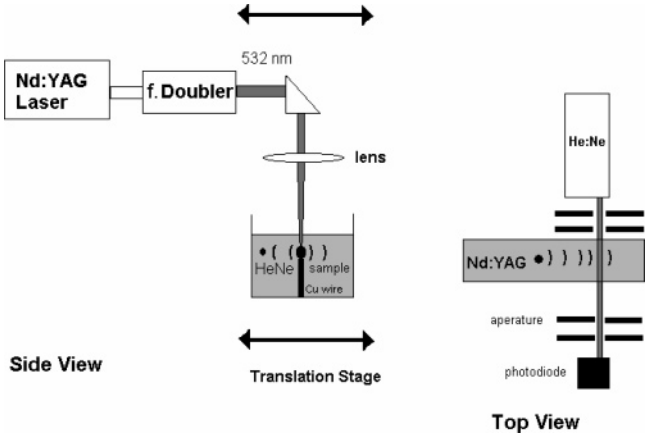

Figure 1. Experimental apparatus for measuring the speed of sound in racemic and optically active MBA.

and NMR spectroscopic studies on solute-MBA mixtures, and optical rotation studies on solute−optically active MBA mixtures.

Experimental Section

Spectroscopic Experiments. Samples of α-Methylbenzylamine (MBA) were obtained from Sigma-Aldrich (>98%). Solutions were prepared by adding appropriate fractional volumes of MBA and solvent measured with a pipet with μL precision. Methanol was HPLC grade (99.9%), cyclohexane was obtained from Aldrich (99.5%), DMSO was obtained from Fisher Scientific (99.9%), nitrobenzene was obtained from Fluka (99.5%), and toluene was HPLC grade (99.9%). Solution concentrations were varied from pure solute ($\chi_{MBA} = 1.0$) to pure solvent ($\chi_{MBA} = 0.0$).

Infrared spectra were recorded on a Bomem DA8 FTIR spectrometer. Small volumes of sample (~1 mL) were compressed between two MgF_2 plates. The IR source was a Globar, and 40 scans were recorded with a resolution of 0.25 cm^{-1}. A spectrum of the atmosphere and MgF_2 plates was recorded for each solvent and utilized as the background when converting to absorbance spectra. NMR spectra were recorded on a Varian 300 MHz spectrometer for protons. For all samples, a two chambered NMR tube was used to hold the sample and reference. Deuterium oxide (Cambridge Isotopes 99.9%) was the reference for all samples and was isolated from the samples to prevent interfering solvent effects. Optical rotations of the prepared solutions were measured on a Perkin-Elmer 241 polarimeter at 25 °C at 589, 578, 546, 436, and 365 nm in a 1 cm cell. All reported optical rotations are the average of 3 or more data points for each concentration. The volumes of MBA with each of the solvents was found to be additive through the addition of known volumes using a microliter pipet.

Quantum Mechanical Calculations. All quantum mechanical calculations were carried out using the Gaussian03[22] suite. Solvated systems were constructed using the polarizable continuum model (PCM). All calculations utilized the B3LYP functional with various basis sets.

Speed of Sound Measurements. The speed of sound measurements were carried out as described in the Results section above using the apparatus shown in Figure 1.

Results

Speed-of-sound measurements and the resulting isoentropic compressiblities have been used as an aid in understanding intermolecular forces.[9,10] Previously two of us reported speed

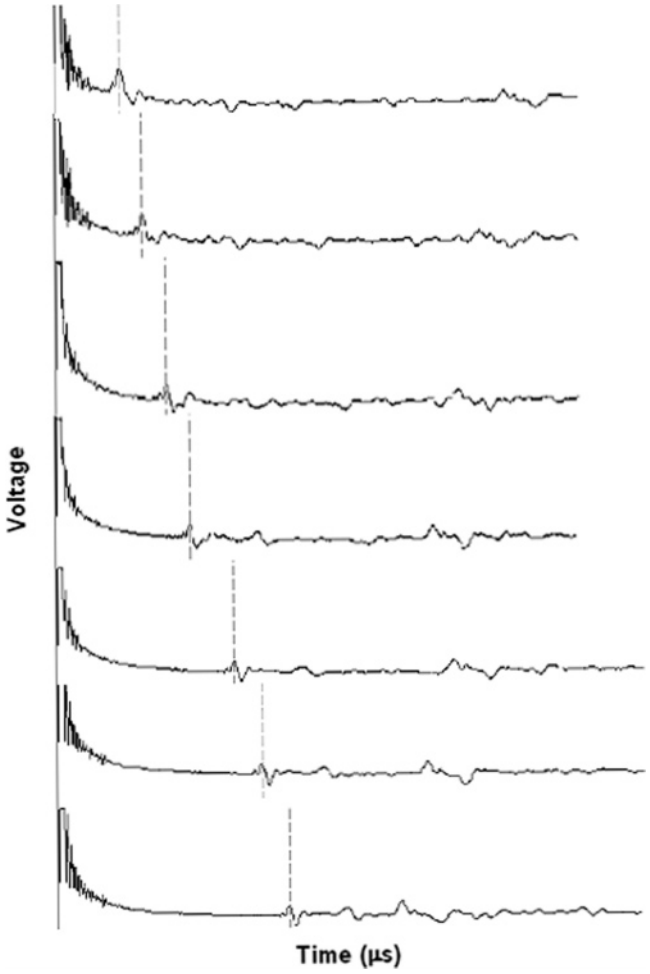

Figure 2. Typical spectra of the speed of sound profile in MBA. The top spectrum represents a distance of 1.250 mm between the two lasers, and each following spectrum has an increased distance of 0.625 mm between the lasers. Structures at times longer than that due to the single pass peak are probably a result of angular reflections in the sample vessel.

of sound measurements of aqueous solutions of D, L, and DL alanine.[11] The isoentropic compressibilites were found to be identical for all three chiral solutions, at all densities. For neat MBA one would expect differences in the speed of sound because the chiral molecules interact directly with one another, without the interference of solvent molecules. Unfortunately, the laser-based method developed earlier[11] to measure the speed of sound in aqueous alanine did not work here because of the considerably higher viscosity and sound absorption in the case of neat MBA. As described in the next two paragraphs, a modification of the previous laser based method was successfully developed to measure the speed of sound.

A technique[11] has been developed that utilizes a laser-induced sound wave to measure the speed of sound in a liquid. Briefly, the technique relies upon focusing a laser into the liquid and inducing a sound wave. A second laser (He:Ne laser) serves as the detector for the sound wave; when the light from the highly collimated He:Ne laser is deflected by the diffraction due to the sound wave from the photodiode detector, an oscilloscope records the time of transit for the sound wave. The entire apparatus is mounted on a translational stage allowing for variation of the distance from the original focal point to the detecting He:Ne beam. A plot of distance versus corresponding time of transit yields a line with the slope being the speed of

sound for the liquid. This methodology has been shown to give results accurate to 0.06% for accepted values of the speed of sound in water.

The apparatus was modified to accommodate the viscous racemic and optically active MBA. The experimental geometry is shown in Figure 1. It was found that the MBA greatly absorbed the sound wave and the focused laser beam could not be employed as the sound source; thus a filament of copper wire was placed into the solution, and the laser was focused onto the tip of the filament to produce an intense sound source. The sample cell was approximately 4 cm in length and 1 cm wide with a depth of 4 cm; the cell was mounted on a translation stage. The position of the translation stage could be changed in increments of 0.080 mm. The detector for the sound wave was a Metrologic He:Ne laser beam that was collimated to a diameter of 0.5 mm before passing through the solution and into a photodiode (ThorLabs Model DET1-SI). The photodiode was triggered with the generation of the light source, and the transit time between the generation of the sound wave to the disturbance of the He:Ne beam was monitored as a function of distance with the mobile stage. The "nominal" time of transit of the sound wave was taken to be the difference between the trigger time and the time at the highest point of the wave pattern. Figure 2 shows a typical set of waveforms of the detected sound waves. The top spectrum represents a distance of 1.250 mm between the two lasers, and each following spectrum has an increased distance of 0.625 mm between the lasers. The features occurring at longer time from the main peak are due to reflections within the sample cell.

The slight offset between the two lines is attributed to the slightly different starting points of the "spark" on the copper wire. This introduces no error since the speed of sound in the liquid is determined from the slope of a best fit line through the plot of the time for the sound wave to travel versus the distance the wave traveled. Attenuation of the sound in the present experiment also affected the quality of data of the present experiment. Using the laser based methodology without the copper tip, the error of the measurements in aqueous alanine and aqueous solutions was accurate to ~0.5%, and the uncertainty of the data herein are similar. Sample plots of distance versus time are shown for R and RS MBA in Figure 3. Table 1 shows data for 18 separate experiments.

The speed of sound in racemic and *S* MBA at 25 °C is 1503.7 ± 4.0 and 1489.8 ± 3.7 m/s, respectively, corresponding to differences in value of about 1%. Equation 1 relates the speed of sound u to the isoentropic compressibility β:

$$\beta = -\frac{1}{V}\left(\frac{\partial V}{\partial P}\right)_S = \frac{1}{\rho u^2} \quad (1)$$

where V, P, S, and ρ represent volume, pressure, entropy and density, respectively. Because the densities of the racemic and optically active MBA are essentially identical (0.949 g/mL), one calculates the isoentropic compressibilites of racemic and optically active MBA to be 4.660 ± 0.012 × 10^{-10} and 4.748 ± 0.011 × 10^{-10} m^2/N, respectively. The compressibilities differ in value by almost 2%. Interestingly, the very slightly denser racemic liquid has the smaller isoentropic compressibility.[12,13] The larger compressibility implies that two *SS* molecules are easier to compress that the *RS* pair. This makes physical sense in that two hands of the same handedness are easier to fit together than two opposite hands.

Rodnikova et al. give an interesting argument for the existence of a three-dimensional hydrogen-bonding network in a variety of liquids based on the magnitudes of their isothermal compressibilities.[10] Liquids such as alkanes where hydrogen bonding is not possible have higher compressibilities than those for which hydrogen bonding is possible, such as alcohols, diols, aminoalcohols, and water. The compressibility of octane, for example, is 16.45 × 10^{-11} m^2/N while that of water is 4.599 × 10^{-11} m^2/N. Hydrogen-bonding plays a significant role in the structure of liquid water. The compressibilities of racemic and *S* MBA are very similar to that of water. The nearly equal compressibilities of water and MBA and the fact that both can donate two hydrogen atoms in hydrogen bonding and accept two (the two lone pairs of electrons on water and the lone pair on nitrogen and possibly the phenyl ring on MBA) strongly suggest that MBA, both in its racemic and optically active forms is held together by a three-dimensional network of hydrogen bonds. One would expect the hydrogen bonds in MBA, especially to the phenyl ring, to be weaker than those in water. Because the partial molar volumes, isoentropic compressibilities, and NH_2 proton chemical shifts[13] are different for racemic and *S* MBA, the hydrogen-bonding networks of the two liquids are subtly different. The viscosity of racemic MBA and the isomeric

TABLE 1: Results for Individual Speed of Sound Experiments (m/s)[a]

racemic MBA (m/s)	S MBA (m/s)	Δ (m/s)
1499.5	1498.3	1.2
1507.5	1489.7	17.8
1508.6	1491.7	16.9
1507.3	1493.3	14.0
1503.7	1487.8	15.9
1507.3	1492.3	15.0
1504.1	1481.8	22.3
1504.1	1490.7	13.4
1499.9	1489	10.9
1507.3	1491.7	15.6
1494.1	1489.1	5.0
1501.0	1485.5	15.5
1505.2	1487.5	17.7
1498.6	1486.3	12.3
1499.1	1488.6	10.5
1506.9	1486.7	20.2
1502.8	1489.7	13.1
1506.0	1491.7	14.3
1506.7	1494.4	12.3

[a] Values are tabulated for both racemic and (*S*)-α-methylbenzylamine. The Δ column highlights the difference between individual experiments. All experiments were at 25 ± 1 °C. The standard deviation of the results is as follows: racemic MBA, $y = 1503.7\ (\pm 4.0)x + 2.22 \times 10^{-4}\ (\pm 9.00 \times 10^{-5})$; S-MBA, $y = 1489.8\ (\pm 3.7)x - 6.70 \times 10^{-5}\ (\pm 4.11 \times 10^{-5})$.

TABLE 2: Selected Parameters of MBA and Five Solutions[a-c]

		Kamlet−Taft			dipole	dielectric
compound	δ/MPa$^{1/2}$	α	β	π^*	moment[d] (D)	constant[d]
MBA	20.1	0.05	0.72	0.81	1.15[e]	5.18[e]
cyclohexane	16.8	0	0	0	0	2.02
toluene	18.2	0	0.11	0.49	0.375	2.385
nitrobenzene	20.5	0	0.30	0.86	4.22	35.6
dimethyl sulfoxide	24.5	0	0.76	1.00	3.96	47.24
methanol	29.6	0.98	0.66	0.60	1.70	33.0

[a] Reichardt, C. *Solvents and Solvent Effects in Organic Chemistry*, 2nd ed.; VCH: Weinheim, Germany, 1990. [b] Marcus, Y. *The Properties of Solvents*; Wiley: Chichester, U.K., 1998. [c] Barton, A. F. M. *Handbook of Solubility Parameters at Other Cohesive Parameters*; CRC Press: Boca Raton, 1983. [d] In *Lange's Handbook of Chemisty*, 15th ed.; Dean, J. A., Ed.; McGraw Hill: New York, 1999. [e] Value for benzylamine.

2-phenylethylamine ($PhCH_2CH_2NH_2$) were measured close to a century ago and are 1.66 cP and 3.07 cP, respectively, at 25 °C.[14] The high values are also consistent with the primary and secondary amines being strongly associated by hydrogen bonding. Interestingly, the viscosity of 2-phenylethylamine is almost twice that of MBA. The NH_2 group in 2-phenylethylamine is in a less sterically demanding environment than the group is in MBA, and thus can form a stronger hydrogen-bonding network.

The behavior of five substrates, cyclohexane, toluene, nitrobenzene, dimethyl sulfoxide (DMSO), and methanol, in MBA was examined as a function of mole fraction by FTIR (asymmetric NH stretch of MBA), proton NMR (solute and solvent), and polarimetry. At low MBA mole fraction, MBA is the solute and the substrates serve as solvent, whereas at high mole fraction of MBA, the designation of solute and solvent is reversed. Table 2 contains selected solvent properties of MBA and its five solutes. The Hildebrand solubility parameters (δ) of the six compounds are sufficiently close to one another that the solutes should be completely miscible in MBA, as was observed. Table 2 also displays the Kamlet-Taft parameters, α (hydrogen-bond donor acidity), β (hydrogen-bond acceptor basicity), and π^* (dipolarity/polarizability), for the six substances. The values for the five solutes are taken from the literature, while those for MBA were estimated from the values for compounds having similar structures to MBA. MBA is polar, a good hydrogen bond acceptor, and a relatively poor hydrogen bond donor. The α, β, and π^* values of the five solutes vary considerably in magnitude, making them excellent test cases for exploring different solvation mechanisms in MBA. Table 2 also contains the dielectric constants and dipole moments of the five substrates and estimates for MBA:

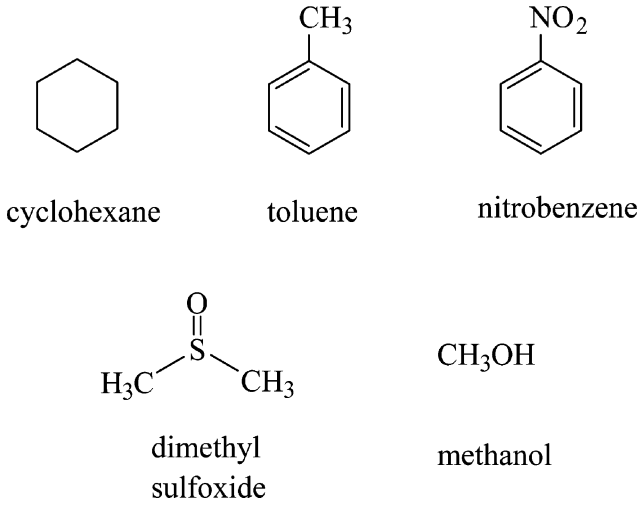

Infrared spectroscopy with its very short time scale is an excellent probe of solvation.[1] Even though only the asymmetric NH stretch of MBA was examined in detail, the stretch will remain distinct, even when MBA is extensively hydrogen bonded to a solute such as methanol. The position of the NH stretch will then reflect intermolecular hydrogen bonding and polarity. Many studies have used nuclear magnetic resonance to probe solute−solvent interactions.[1,15] Proton NMR, even though it has a long time scale, has the advantage that one can measure the chemical shifts of both solute and solvent. NMR was used in this study to complement the IR studies. We previously have examined the influence of the Kamlet-Taft parameters on the specific rotation of optically active MBA in solution. In the present study polarimetry was used in a different fashion. The rotation of *S* MBA was studied as a function of the mole fraction (and molarity) of the five MBA-solute combinations. As described elsewhere,[16] this represents a method for examining nonideal behavior of optically active substrates in solution.

TABLE 3: Asymmetric NH Stretch of MBA in Five Solutions as a Function of Mole Fraction

	cyclohexane	toluene	nitrobenzene	methanol	DMSO
χMBA[a]	νasy (cm^{-1})	νasy (cm^{-1})	νasy (cm^{-1})	νasy (cm^{-1})	νasy (cm^{-1})
1.0	3366.5	3366.5	3366.5	3366.5	3366.5
0.9	3366.8	3368.1	3367.1	3364.3	3363.9
0.8	3367.7	3369.5	3369.3	3361.6	3365.4
0.7	3367.9	3370.3	3371.2	3357.1	3361.4
0.6	3369.3	3371.5	3372.8	3353.2	3359.9
0.5	3370.3	3373.4	3374.5	3357.2	3359.2
0.4	3370.4	3375.8	3376.7	3349.3	3358.7
0.3	3372.3	3377.4	3378.2	3346.9	3356.9
0.2	3380.7	3379.9	3379.6	3343.8	3356.8
0.1	3439.4	3381.5	3380.9	3344.0	3353.8
νasy [0 b]	3583.6	3382.2	3380.6	3345.6	3349.2
νasy[calcd. c]	3531	3522	3459	3457	3454

[a] Mole fraction of MBA. [b] Extrapolated infinite dilution value. [c] Calculated value (PCM methodology utilizing B3LYP functional with aug-cc-pVDZ basis set). Takes into account the dielectric constant of the solvent.

In Figure 4 is plotted the specific rotation of *S* MBA in mixtures of the five substrates as a function of MBA mole fraction (χ_{MBA}). The top two sets of data represent the behavior of methanol and DMSO. Here the specific rotation decreases significantly as the mole fraction of MBA increases. The bottom three sets of data represent the behavior of cyclohexane, nitrobenzene, and toluene. In these latter three cases the specific rotations do no change much as a function of mole fraction. At low χ_{MBA}, the five compounds represent solvents, with MBA serving as solute; the corresponding specific rotations, which go from roughly −60° to −80°, reflect indirectly the solvation of MBA by the five compounds by MBA. This is similar to what was observed in our previous study.[8] In Figure 5 is plotted the observed rotation of *S* MBA in solute-MBA mixtures as a function of χ_{MBA}. Careful analysis of the data shows that the cylohexane, toluene and nitrobenzene curves are linear while those for methanol and DMSO have convex shapes. A similar plot (not shown) for observed rotation versus molarity reveals that the cylohexane, toluene and nitrobenzene curves are likewise linear and those for methanol and DMSO are concave.

What do the data in Figures 4 and 5 imply? As described elsewhere, the observed rotation of a solute should be linear in molar concentration, at low concentrations of solute.[16] This is the polarimetry equivalent of Beer's Law. At higher concentration one would expect deviations from linearity because the liquid mixture becomes dominated by the solute, not the solvent. At higher concentrations of solute one might also see solute−solute interactions which could affect the observed rotation as well. Surprisingly, three of the solute−MBA plots are linear through the entire concentration regime. Even though the MBA three-dimensional hydrogen-bonding network must be perturbed at high concentrations of the three solutes, this is not reflected in the optical rotations. One way in which this can be envisioned is if a hydrogen-bonded MBA molecule has roughly the same rotation as an MBA monomer. In other words, any breakup of the network does not alter the rotation of the MBA units in the mixtures containing cyclohexane, toluene, and nitrobenzene. On the other hand, the methanol and DMSO curves are decidedly nonlinear, suggesting a strong interaction between these two molecules and MBA. These are the two molecules where

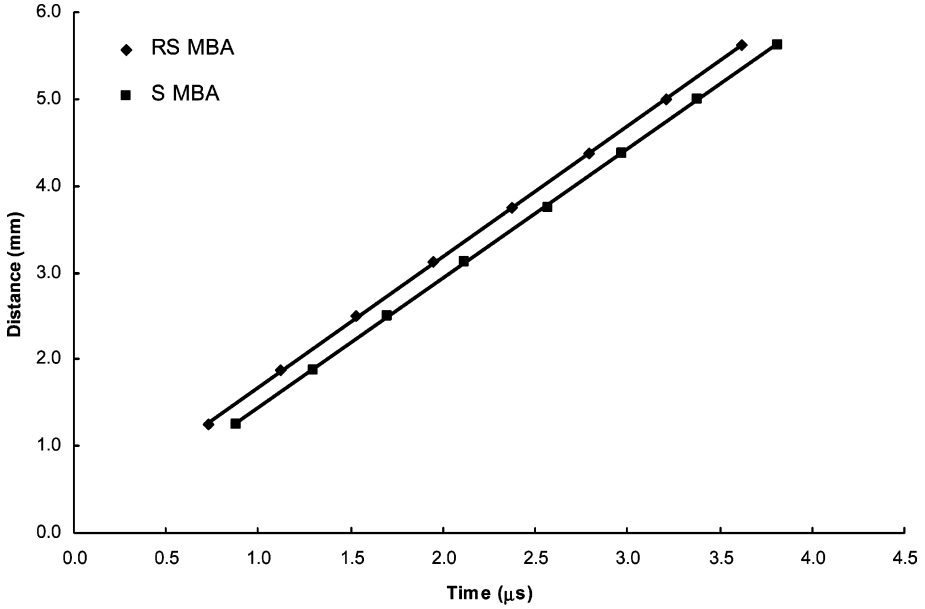

Figure 3. Sample plots of the distance versus time for both the *RS* and *R* samples are shown. The offset is a result of a different focal spot on the copper wire inducing the sound wave.

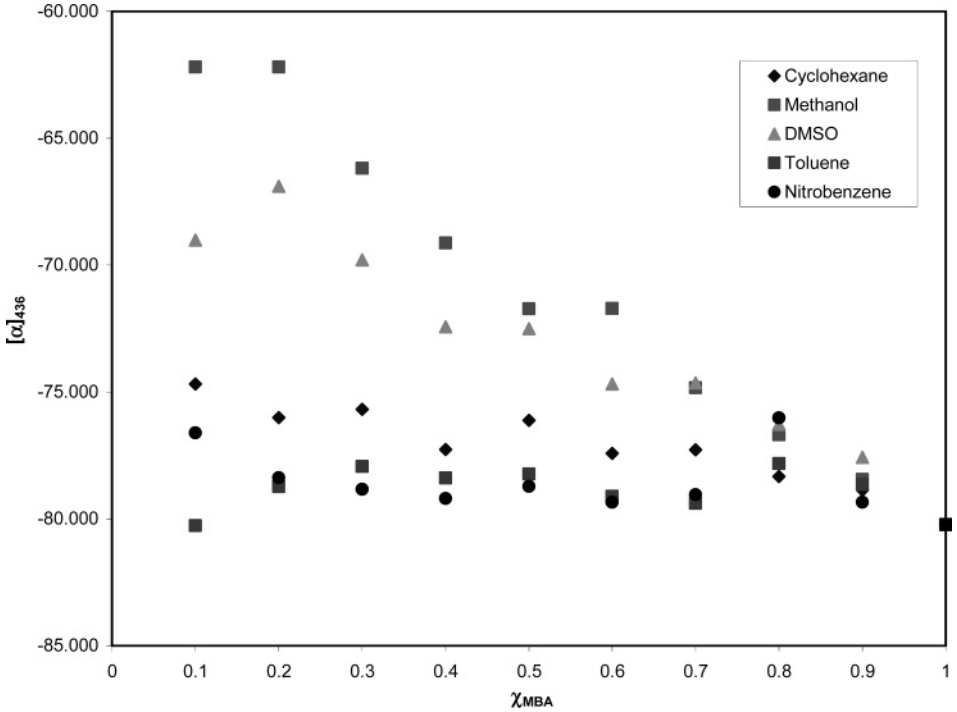

Figure 4. Specific rotations of *S*-MBA at 436 nm as a function of the mole fraction of MBA in five solvent.

hydrogen bonding between substrate and MBA should be the most significant.

Table 3 summarizes the results of the FTIR experiments on mixtures of racemic MBA and the five solutes/substrates. The asymmetric NH stretch[17] was measured in all five cases as a function of χ_{MBA}. The extrapolation of the NH stretch to infinite dilution of MBA was also determined. The extrapolated value was also calculated by molecular orbital methods which take into account the dielectric constant of the five substrates. The same calculations on the optimized MBA also afforded Mullikan charges of the amine in the gas phase and the five substrates; these are shown in Table 4. The extrapolated NH stretches, of course, reflect MBA as solute. The manner in which MBA is solvated by a substrate provides clues on how the substrate is solvated by MBA. The results from our earlier study[8] are also useful in this regard. Each IR data set was complimented by a corresponding ^{1}H NMR data set of chemical shifts of MBA and substrate as a function of χ_{MBA}. These are shown in Figures 6-10. Note that it was not possible to determine every chemical shift to its extreme value because peaks often became too weak in intensity to detect.

Let us first consider the combination of cyclohexane and MBA. In Figure 6 is shown the chemical shifts of the NH_2, CH_3, and CH protons of MBA as well as that of cyclohexane. There is a slow monotonic change to higher shielding in all four cases as the amount of MBA increases. These changes undoubtedly reflect the significant change in polarity (Table 2) in going from $\chi_{MBA} = 0$ to 1, keeping in mind that the data

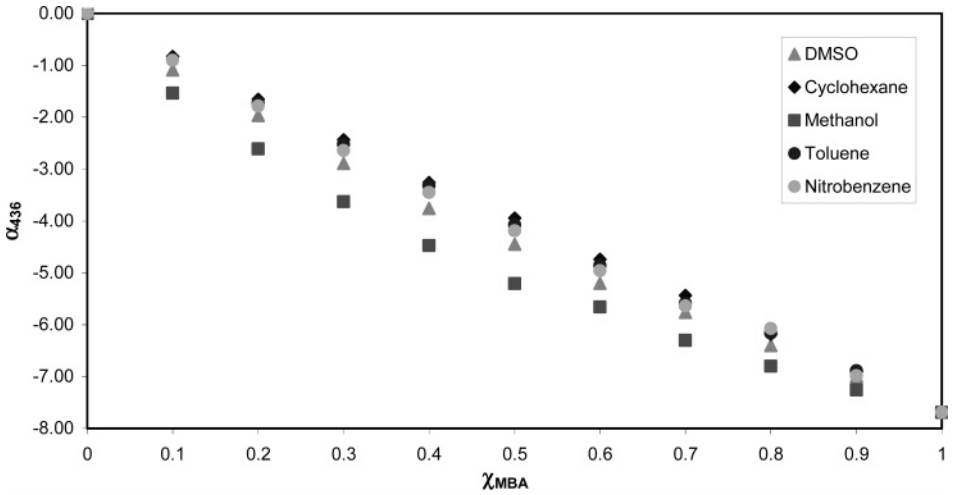

Figure 5. Observed rotation of *S*-MBA at 436 nm as a function of the mole fraction of MBA in five solvents.

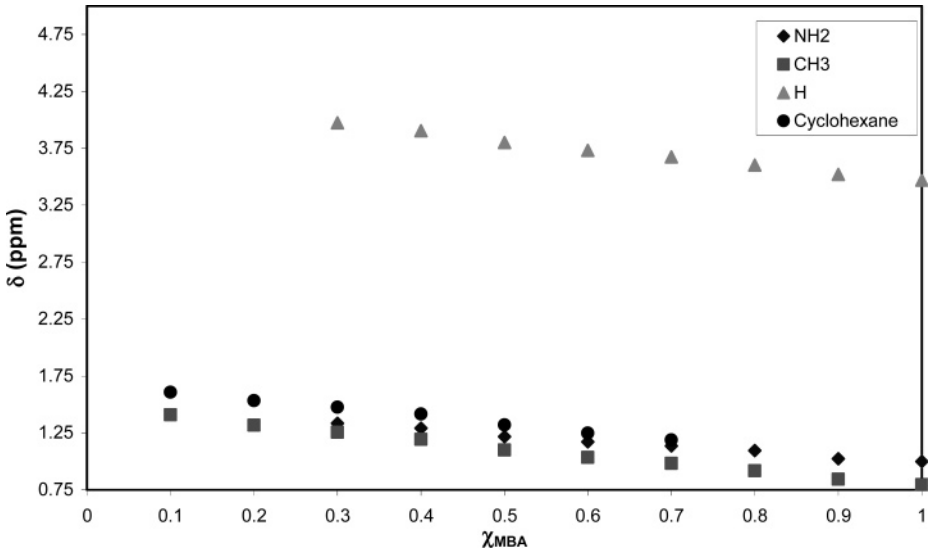

Figure 6. ^{1}H NMR chemical shifts of MBA and cyclohexane as a function of the mole fraction of MBA.

TABLE 4: Selected Mullikan Charges on Optimized MBA in the Gas Phase and Five Substrates

	phase						
atom(s)	gas	cyclohexane	toluene	nitrobenzene	dimethyl sulfoxide	methanol	MBA and methanol[a]
nitrogen	0.07	0.03	0.02	−0.05	−0.07	−0.06	−0.51
chiral carbon	0.29	0.32	0.35	0.37	0.40	0.39	0.37
methyl carbon	1.03	1.02	1.00	1.01	0.99	0.99	1.13
methine H	−0.61	−0.60	−0.61	−0.59	−0.60	−0.60	−0.66
methyl H's	−0.28	−0.28	−0.28	−0.28	−0.28	−0.28	−0.30
amines H's	−0.11	−0.09	−0.09	−0.06	−0.07	−0.07	−0.13

[a] Methanol hydrogen bonded to MBA as seen in Figure 11.

were not corrected for bulk magnetic susceptilibity. The IR data were very informative. There is a very small upward shift in the position of the NH stretch in neat MBA to its value in 30:70 MBA:cyclohexane (about 6 cm^{-1}) at which point a dramatic change occurs. Between 30:70 MBA:cyclohexane and neat cyclohexane the position of the NH stretch changes by over 210 cm^{-1}. The experimental extrapolated value in pure cyclohexane is very similar to that calculated theoretically which takes into account the dielectric constant of the hydrocarbon.

What do the above data signify? In MBA, dilute solutions of cyclohexane interact with MBA solvent by dispersion and dipole−induced dipole forces; cyclohexane has no effect on the three-dimensional hydrogen-bonding network of MBA. In fact, the hydrogen-bonding network remains largely intact, even in solutions with 70 mol % cyclohexane. Somehow the non-interacting cyclohexane with α, β, and π^* values of 0 is able to squeeze into MBA without breaking the hydrogen bonds. When 70 mol % is reached, there is so much hydrocarbon present that the hydrogen-bonding network breaks apart and the NH stretch is influenced at this point by the polarity of the mixture of the two compounds, one polar (MBA) and the other not (cyclohexane). The OD stretch of CH_3OD is known to be influenced by polarity in the same direction.[18] In cyclohexane the MBA molecule is isolated and feels the full force of the hydrocarbon's dielectric constant. This is reflected in the fact that the calculated NH stretch is in reasonably good agreement

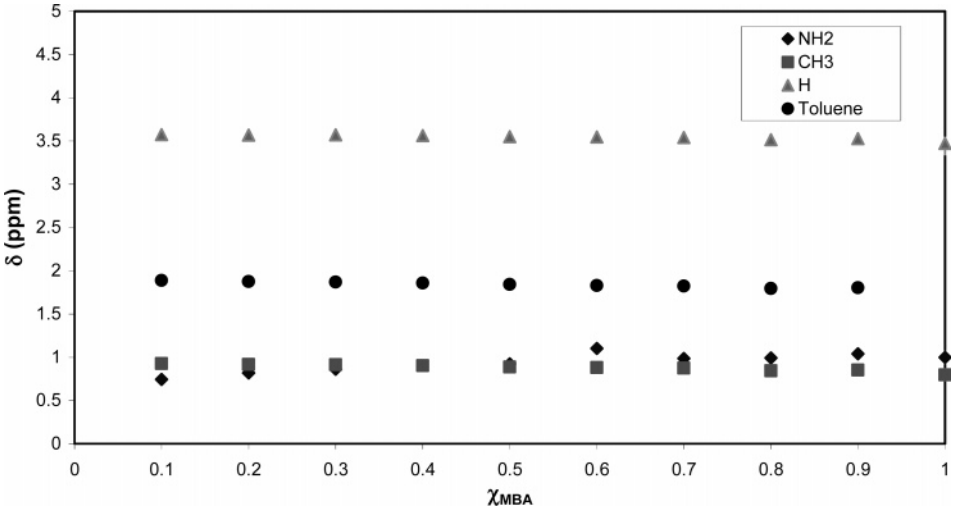

Figure 7. [1]H NMR chemical shifts of MBA and toluene as a function of the mole fraction of MBA.

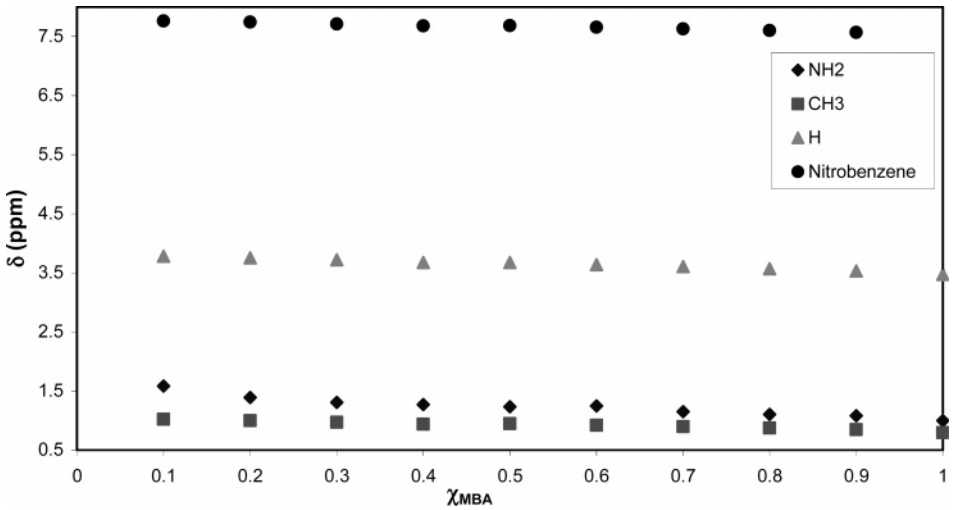

Figure 8. [1]H NMR chemical shifts of MBA and nitrobenzene as a function of the mole fraction of MBA.

with the experimental value. In cyclohexane, MBA interacts with the solvent through dispersion and dipole-induced dipole forces. There is no specific interaction of the NH hydrogen with cyclohexane.

Figures 7 and 8 display the NMR data for the toluene- and nitrobenzene-MBA mixtures, respectively. For toluene, its methyl chemical shifts are displayed while, for nitrobenzene, its aromatic chemical shifts are shown. For MBA, its NH_2, CH_3, and CH protons are shown, as before. In both sets of data there is a very slight increase in shielding for each substituent as the mole fraction of MBA is increased. The effect is much smaller than seen for cyclohexane−MBA where the difference in polarity of the two components is very large. The FTIR data show similar trends as well. The position of the NH stretch increases by 14−16 wavenumbers in both cases in going from pure MBA to pure substrate. Interestingly, the calculated limiting NH stretch which takes into account the dielectric constant of the medium is off by 140 wavenumbers for toluene and almost 80 wavenumbers for nitrobenzene. These differences are larger than seen in the case of cyclohexane. The calculations do not take into account that, when MBA functions as solute, the molecule can donate a hydrogen bond to the π bonds of both toluene and nitrobenzene (small α for MBA matched with a larger β for the aromatic substrates). All three substrates have significant π^* values so that solvation via dipole−dipole interactions is likely. $\pi-\pi$ stacking, facilitated by hydrogen bonding between MBA and substrate may also occur. When toluene and nitrobenzene are solutes in MBA, the same mechanisms of solvation operate: hydrogen bonding between solute and solvent, dipole−dipole interactions, and $\pi-\pi$ stacking. Both substrates, unlike cyclohexane, with their modest to good β values, undoubtedly begin to break up the three-dimensional hydrogen-bonding network of MBA at very low concentrations.

The results of the NMR experiments on DMSO-MBA mixtures are displayed in Figure 9. For DMSO the chemical shifts of its methyl groups are shown. Although all the behavior of all the peaks is the same, i.e., moving to higher field on going from $\chi_{MBA} = 0$ to 1, the effect is most dramatic for the NH_2 resonance where there is close to a 2.5 ppm change in position. Based on the fact that MBA and DMSO have similar β values it is likely that the NH_2 chemical shift is a weighted average between MBA hydrogen bonded to itself and MBA hydrogen bonded to the oxygen of DMSO. The FTIR results show a small decrease in going from $\chi_{MBA} = 0$ to 1. The frequency of the NH stretch when it is bonded to itself is likely to be similar in value to the stretch when it is hydrogen bonded to DMSO. The extrapolated and theoretical values for the limited NH stretch vary by over 100 wavenumbers, a consequence of the fact that the theoretical calculation does not take into account hydrogen bonding. Thus, when MBA is a solute in DMSO, the primary mode of solvation is via relatively strong hydrogen bonding.

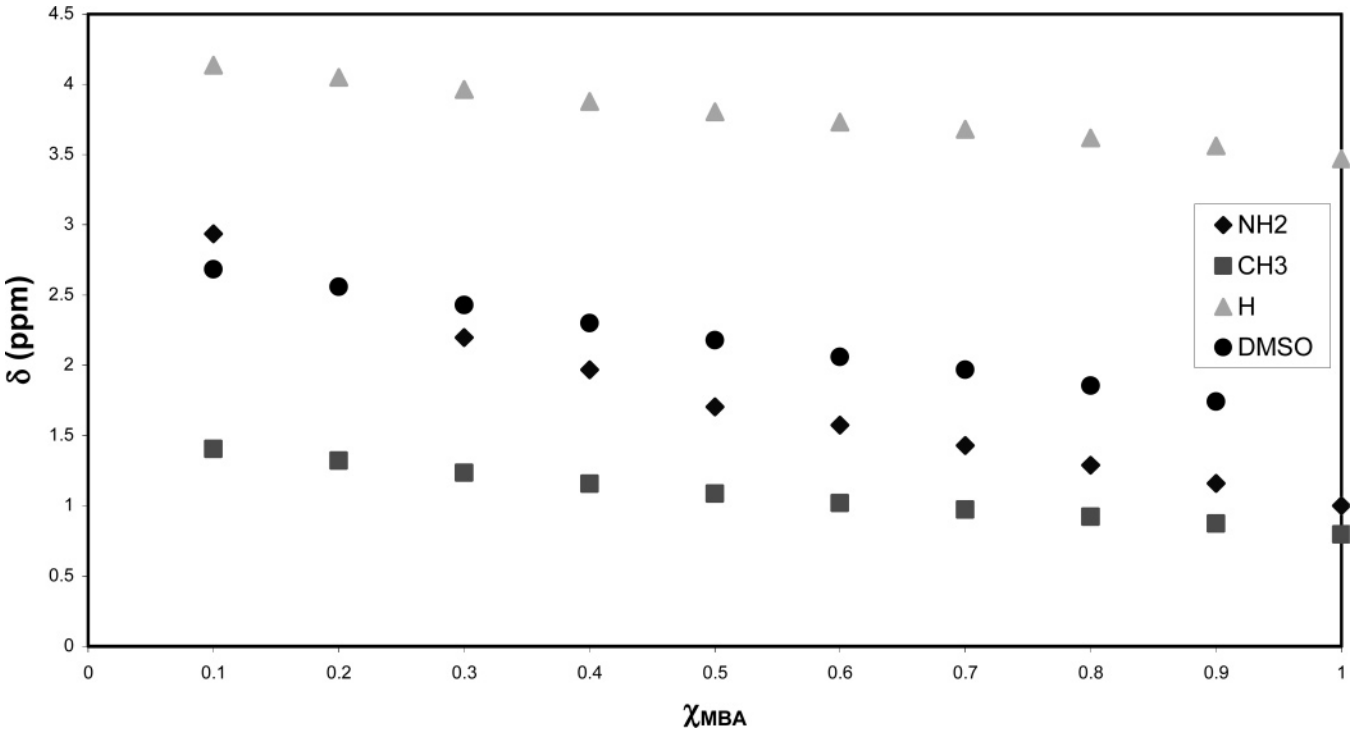

Figure 9. [1]H NMR chemical shifts of MBA and DMSO as a function of the mole fraction of MBA.

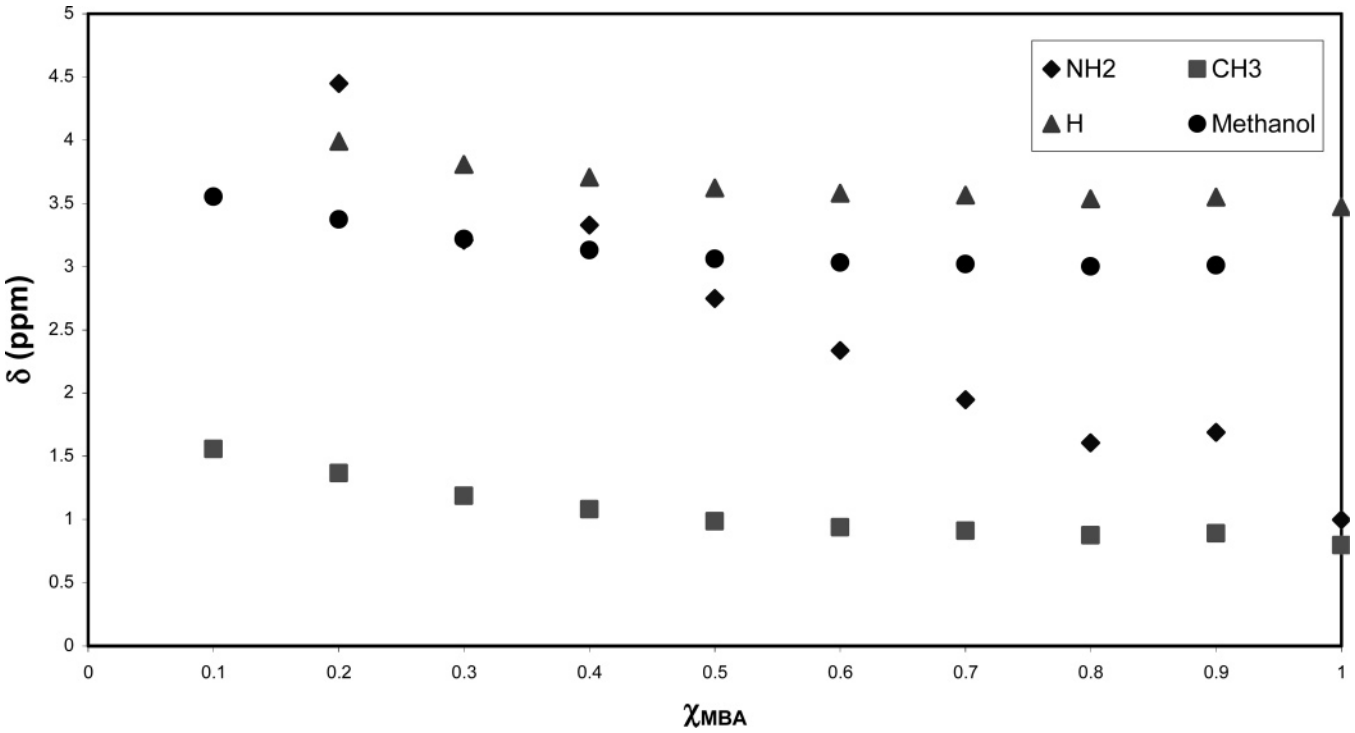

Figure 10. [1]H NMR chemical shifts of MBA and methanol as a function of the mole fraction of MBA.

Dipole−dipole interactions between polar MBA and very polar DMSO undoubtedly also are involved in solvation. When DMSO is the solute, similar modes of interaction with MBA operate as well.

Figure 10 shows the proton NMR data for MBA−methanol mixtures. The chemical shifts of three functional groups on MBA, NH_2, CH_3, and CH are seen, as in the previous four figures. The CH_3 chemical shift of methanol is also displayed. The shifts labeled as belonging to NH_2, which change by over 4 ppm from one end of the mole fraction scale to the other, are in fact those for NH_2 and the OH of methanol. One way in which this is apparent is that the peak integrates for three hydrogens. The two amino and one hydroxyl hydrogen atoms are undergoing rapid exchange on the NMR time scale. The observed chemical shift is then a weighted average of the OH chemical shift of methanol and the NH_2 chemical shift of MBA. The FTIR data for methanol-MBA (Table 3) are very similar to that of DMSO−MBA in every respect. What distinguishes methanol from the other four substrates is that it is an excellent hydrogen bond donor as attested by its large α value (Table 2). MBA is an excellent hydrogen bond acceptor as seen by its large β value. The conclusion then is that the

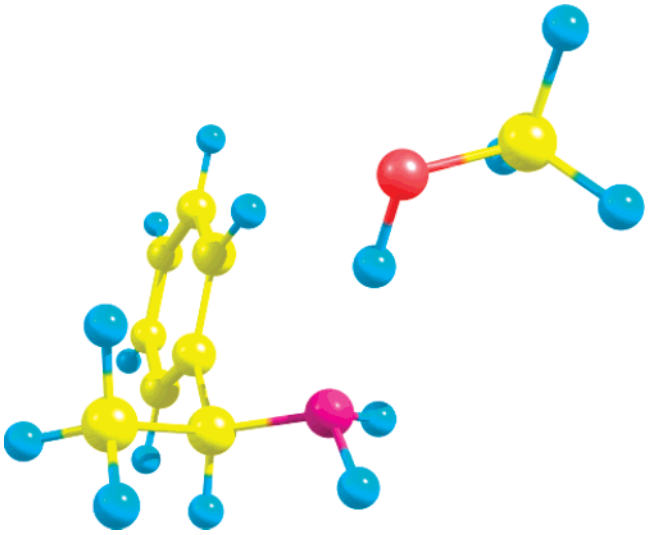

Figure 11. Optimized structure of the MBA-methanol dimer in methanol which was calculated using PCM B3LYP functional and aug-cc-pVDZ basis set.

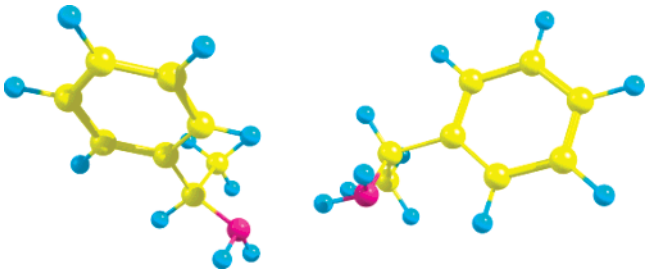

Figure 12. Optimized structure of the MBA dimer in methanol which was calculated with PCM B3LYP methodology with a cc-pVDZ basis set.

primary mode of interaction between methanol and MBA is via hydrogen bonding from the alcohol hydroxyl group to the nitrogen atom of MBA. This is equally true when MBA is a solute in methanol and when methanol is a solute in MBA. Methanol is even more effective in breaking up the hydrogen-bonding network of MBA than is DMSO. A molecular orbital calculation was carried out in which an MBA molecule is allowed to interact with a methanol molecule. The results of the calculation, shown in Figure 11, clearly reveal the hydrogen bond from the alcohol to the amine.

Concluding Remarks

Figure 12 displays the calculated structure of the MBA dimer (in methanol). Two things are apparent from the structure: the dimer is held together with an NH to N hydrogen bond and the large phenyl and methyl groups of one MBA unit are opposed to those in the other unit. It is not difficult to envision these features being extended in each direction by further hydrogen bonds, thus yielding a columnar structure for the liquid. This picture neglects any hydrogen bonding to the benzene ring. This secondary hydrogen-bonding could be accomplished by a non-hydrogen-bonding NH bond in one column interacting with a benzene ring in a second column. If many hydrogen bonds of this type were formed, one would obtain a three-dimensional lattice of hydrogen bonds, some from NH bonds to nitrogen atoms and others to benzene rings.

Zingg et al. have reported results on a study on the interaction between the *R* enantiomer of MBA and the *R* and *S* enantiomers of mandelic acid.[19] Extensive experimental work by these researchers shows that the resulting diastereomeric ion pairs are subtly different in structure, one being held together via a single hydrogen bond from NH on the cation to the carboxyl group on the anion and the other by two such hydrogen bonds. Although the example of MBA is different in many respects from the Zingg cases, racemic and *S* MBA may form diastereomeric hydrogen-bonded dimers which are likewise subtly different in structure. The models that Zingg et al. propose for their diastereomeric ion pairs have the benzene ring of the cation sitting over the benzene ring of the anion, thus encouraging $\pi-\pi$ interactions. $\pi-\pi$ interactions may also be important in the structure of liquid MBA, although we feel that hydrogen bonding from NH to benzene to be more important.

The behavior of cyclohexane in MBA is particularly interesting. Liquid MBA is able to adjust its structure to hold considerable amounts of cyclohexane without disrupting the three-dimensional hydrogen-bonding network. Both toluene and nitrobenzene interact with MBA differently. Hydrogen bonding from MBA to the aromatic rings of the two substrates is important as are dipole−dipole interactions and perhaps $\pi-\pi$ interactions between the aromatic rings of substrate and solvent. DMSO is known to form hydrogen bonds with amines[20] and alcohols.[21] This behavior is particularly evident in our system by the optical rotation and NMR data. DMSO is able to break up the hydrogen-bonding network of liquid MBA and replace it with hydrogen bonds of a different character, from NH on the amine to the oxygen on DMSO. Because MBA and DMSO are both polar molecules, dipole−dipole interactions between solute and solvent are also important. Methanol also interacts with MBA via hydrogen bonding. This is evident from polarimetry data and especially the NMR data which strongly suggest that the two NH hydrogen atoms of MBA rapidly exchange with the one OH hydrogen atom of the alcohol. What is distinctive about methanol is that it is an excellent hydrogen bond donor which is not true of the other four solutes. Thus, methanol interacts with MBA both by receiving a hydrogen bond from the amine but also by donating one to the amine. Because methanol is a far superior hydrogen bond donor than MBA, and both have comparable hydrogen bonding accepting properties, the primary interaction between the alcohol and amine is via donation from the alcohol to the amine.

Chiral liquids have rarely proven useful in catalyzing asymmetric reactions. This is undoubtedly the case because the solvents interact poorly with the reactants. Chiral liquids such as *S* MBA may be superior in this regard because, with suitable solutes of the type described in this study, solute−solvent interactions may be significant.

Acknowledgment. The authors thank the National Science Foundation for support of this work. Jeffrey Steill assisted with the FTIR measurements.

References and Notes

(1) Reichardt, C. *Solvents and Solvent Effects in Organic Chemistry*, 3rd ed.; VCH: Weinheim, Germany, 2003.

(2) Atik, Z.; Ewing, M. B.; McGlashan, M. L. *J. Phys. Chem.* **1981**, *85*, 3300−3303.

(3) Lepori, L.; Mengheri, M.; Mollica, V. *J. Phys. Chem.* **1983**, *87*, 3520−3525.

(4) Brock, C. P.; Schweizer, W. B.; Dunitz, J. D. *J. Am. Chem. Soc.* **1991**, *113*, 9811−9820.

(5) Atik, Z.; Ewing, M. B.; McGlashan, M. L. *J. Chem. Thermodyn.* **1983**, *15*, 159−163.

(6) Kimura, T.; Khan, M. A.; Ishii, M.; Ueda, K.; Matsushita, T.; Kaiyama, T.; Fujisawa, M. *J. Chem. Thermodyn.* **2006**, *38*, 1042−1048.

(7) Atik, Z.; Saito, Y.; Kusano, K. *J. Chem. Thermodyn.* **1987**, *19*, 99−102.

(8) Fischer, A. T.; Compton, R. N.; Pagni, R. M. *J. Phys. Chem. A* **2006**, *110*, 7067−7071.

(9) Douhéret, G.; Davis, M. I.; Reis, J. C. R.; Blandamer, M. J. *Chem. Phys. Chem.* **2001**, *2*, 148−161.

(10) Rodnikova, M. N.; Val'kovsskaya, T. M.; Kartez, V. N.; Kayumova, D. B. *J. Mol. Liq.* **2003**, *106*, 219−222.

(11) Fischer, A. T.; Compton, R. N. *Rev. Sci. Instrum.* **2003**, *74*, 3730−3734.

(12) Low-frequency vibrational spectroscopy may also yield information about intermolecular interactions. Unfortunately the peak of interest was identical in both the racemic and optically active liquids (143 cm^{-1}).

(13) The NH_2 protons in the ^1H nmr spectra of racemic and *S* MBA have different chemical shifts, 1.101 and 1.124 ppm, respectively.

(14) Mussell, A. G.; Thole, F. B.; Dunstan, A. E. *J. Chem. Soc. Trans.* **1912**, *101*, 1008−1016.

(15) For example, Yoshida, K.; Yamaguchi, T.; Adachi, T.; Otomo, T.; Matsuo, D.; Takamuku, T.; Nishi, N. *J. Chem. Phys.* **2003**, *119*, 6132−6142.

(16) Springer, G. H. MS Thesis, University of Tennesse 1997.

(17) Nakanishi, K. *Infrared Absorption Spectroscopy*; HoldenDay: San Francisco, 1962.

(18) Burden, A. G.; Collier, G.; Shorter, J. *J. Chem. Soc., Perkin Trans. II* **1976**, 1627−1632.

(19) Zingg, S.; Arnett, E.; McPhail, A.; Bothner-By, A.; Gilkerson, W. *J. Am. Chem. Soc.* **1988**, *110*, 1565−1580.

(20) Madec, C.; Lauransan, J.; Saumagne, P. *J. Phys. Chem.* **1971**, *75*, 1157−1162.

(21) Li, Q.; Wu, G.; Yu, Z. *J. Am. Chem. Soc.* **2006**, *128*, 1438−1439.

(22) Frisch, M. J.; Trucks, G. W.; Schlegel, H. B.; Scuseria, G. E.; Robb, M. A.; Cheeseman, J. R.; Montgomery, J. A., Jr.; Vreven, T.; Kudin, K. N.; Burant, J. C.; Millam, J. M.; Iyengar, S. S.; Tomasi, J.; Barone, V.; Mennucci, B.; Cossi, M.; Scalmani, G.; Rega, N.; Petersson, G. A.; Nakatsuji, H.; Hada, M.; Ehara, M.; Toyota, K.; Fukuda, R.; Hasegawa, J.; Ishida, M.; Nakajima, T.; Honda, Y.; Kitao, O.; Nakai, H.; Klene, M.; Li, X.; Knox, J. E.; Hratchian, H. P.; Cross, J. B.; Bakken, V.; Adamo, C.; Jaramillo, J.; Gomperts, R.; Stratmann, R. E.; Yazyev, O.; Austin, A. J.; Cammi, R.; Pomelli, C.; Ochterski, J. W.; Ayala, P. Y.; Morokuma, K.; Voth, G. A.; Salvador, P.; Dannenberg, J. J.; Zakrzewski, V. G.; Dapprich, S.; Daniels, A. D.; Strain, M. C.; Farkas, O.; Malick, D. K.; Rabuck, A. D.; Raghavachari, K.; Foresman, J. B.; Ortiz, J. V.; Cui, Q.; Baboul, A. G.; Clifford, S.; Cioslowski, J.; Stefanov, B. B.; Liu, G.; Liashenko, A.; Piskorz, P.; Komaromi, I.; Martin, R. L.; Fox, D. J.; Keith, T.; Al-Laham, M. A.; Peng, C. Y.; Nanayakkara, A.; Challacombe, M.; Gill, P. M. W.; Johnson, B.; Chen, W.; Wong, M. W.; Gonzalez, C. and Pople, J. A. *Gaussian 03*, Revision C.02; Gaussian, Inc.: Wallingford, CT, 2004.